Pflugers Arch - Eur J Physiol (2002) 444:411–418
DOI 10.1007/s00424-002-0819-8

ORIGINAL ARTICLE

**Siegfried Waldegger · Nikola Jeck · Petra Barth
Melanie Peters · Helga Vitzthum · Konrad Wolf
Armin Kurtz · Martin Konrad
Hannsjörg W. Seyberth**

Barttin increases surface expression and changes current properties of ClC-K channels

Received: 15 January 2002 / Revised: 1 February 2002 / Accepted: 6 February 2002 / Published online: 9 April 2002

Abstract The term Bartter syndrome encompasses a heterogeneous group of autosomal recessive salt-losing nephropathies that are caused by disturbed transepithelial sodium chloride reabsorption in the distal nephron. Mutations have been identified in the NKCC2 (Na^+-K^+-$2Cl^-$) cotransporter and ROMK potassium channel, which cooperate in the process of apical sodium chloride uptake, and ClC-Kb chloride channels, which mediate basolateral chloride release. Recently, mutations in barttin, a protein not related to any known ion transporter or channel, were described in BSND, a variant of Bartter syndrome associated with sensorineural deafness. Here we show that barttin functions as an activator of ClC-K chloride channels. Expression of barttin together with ClC-K in *Xenopus* oocytes increased ClC-K current amplitude, changed ClC-K biophysical properties, and enhanced ClC-K abundance in the cell membrane. Co-immunoprecipitation revealed a direct interaction of barttin with ClC-K. We performed in situ hybridization on rat kidney slices and RT-PCR analysis on microdissected nephron segments to prove co-expression of barttin, ClC-K1 and ClC-K2 along the distal nephron. Functional analysis of BSND-associated point mutations revealed impaired ClC-K activation by barttin. The results demonstrate regulation of a CLC chloride channel by an accessory protein and indicate that ClC-K activation by barttin is required for adequate tubular salt reabsorption.

Keywords Bartter syndrome · BSND · Chloride channels · Deafness · Kidney disorder · Membrane protein · Tubulopathy

S. Waldegger (✉) · N. Jeck · P. Barth · M. Peters · M. Konrad
H.W. Seyberth
Department of Pediatrics, Philipps University of Marburg,
Deutschhausstr. 12, 35033 Marburg, Germany
e-mail: siegfried.waldegger@mailer.uni-marburg.de
Tel.: +49-6421-2862649, Fax: +49-6421-2868956

H. Vitzthum · K. Wolf · A. Kurtz
Department of Physiology I, University of Regensburg,
93040 Regensburg, Germany

Introduction

The diagnosis Bartter syndrome comprises a spectrum of autosomal recessive salt-losing kidney disorders that manifest with chronic hypokalemia and metabolic alkalosis. Renal salt wasting is caused by impaired transepithelial sodium chloride transport in the thick ascending limb of Henle's loop and more distal nephron segments. In epithelial cells of the thick ascending limb (TAL) apical sodium chloride uptake is driven by the sodium-potassium-chloride co-transporter NKCC2. Potassium ions recirculate into the tubular lumen via apical ROMK potassium channels, while chloride is released basolaterally through ClC-Kb chloride channels. Mutations associated with the more severe antenatal variant of Bartter syndrome (also termed hyperprostaglandin E syndrome) have been identified in the genes encoding for ROMK and NKCC2 [15, 16], whereas the less severe classic variant of Bartter syndrome is caused by mutations in ClCNKB encoding for ClC-Kb [14]. Although this genetic evidence convincingly suggests chloride channel function for ClC-Kb, electrophysiological analysis of ClC-Kb upon heterologous expression did not reveal chloride currents [7, 23]. This also applies to ClC-Ka [7], a highly related homologue whose involvement in renal transepithelial chloride reabsorption is suggested by reduced vectorial chloride transport along the thin ascending limb of Henle's loop in a knock-out mouse model for ClC-K1 (the corresponding mouse orthologue) [8]. Thus, the existence of additional factors regulating ClC-K channel activity has been postulated.

Recently, mutations in a new gene (*BSND*) were identified in a Bartter variant called BSND, which, in contrast to the other forms, is associated with sensorineural deafness (SND) and renal failure [2]. The *BSND*-encoded protein barttin shows no homology to any known protein. It has two predicted transmembrane domains and is highly expressed in the distal nephron and in endolymph-producing cells of the inner ear. The BSND phenotype together with the reported tissue distribution suggested barttin as an attractive candidate for a regulatory

ClC-K subunit. We therefore cloned barttin from a human kidney cDNA library and performed co-expression studies with ClC-Kb and ClC-Ka in *Xenopus* oocytes. Electrophysiological analysis indeed revealed activation of ClC-Kb and ClC-Ka chloride currents. The biophysical properties of rat ClC-K1, the only ClC-K homologue which by itself is amenable to functional expression in *Xenopus* oocytes [19, 23], changed after co-expression with barttin. Immunostaining demonstrated an increased membrane abundance of epitope-tagged ClC-K constructs in the presence of barttin, which immunoprecipitated ClC-K from oocyte lysates. Moreover, we determined the intracellular localization of the barttin C-terminus, investigated co-localization of barttin with ClC-K1 and ClC-K2 along the rat nephron, and analyzed the effect of BSND-associated point mutations on ClC-K1 activation by barttin.

Materials and methods

Expression in *Xenopus laevis* oocytes and voltage-clamp analysis

Five nanograms of in-vitro-transcribed cRNA (mMessage mMachine kit; Ambion, AMS Biotechnology, Wiesbaden, Germany) for each construct was injected in defolliculated *Xenopus* oocytes, which were kept at 16°C in ND96 solution containing 96 mM NaCl, 2 mM KCl, 1.8 mM $CaCl_2$, 1 mM $MgCl_2$, 5 mM HEPES (pH 7.4). Two to five days after injection, two-electrode voltage-clamp measurements were performed at room temperature with a GeneClamp 500 amplifier (Axon Instruments, Union City, USA). Currents were recorded in ND96 solution. For anion replacement experiments, 80 mM chloride was substituted by equivalent amounts of the indicated anions. The extracellular calcium concentration was varied by adding calcium acetate to the ND96 solution. Data from at least two different batches of oocytes are shown. Statistical analysis was performed on *n* oocytes derived from one preparation. The error bars in the diagrams were calculated from the standard error of the mean (SEM). Site-directed mutagenesis was performed with the QuickChange system (Stratagene, Amsterdam, The Netherlands) and the complete constructs were sequenced to prove the desired nucleotide exchange and to exclude any additional mutations.

Immunostaining and co-immunoprecipitation

MDCK cells transiently transfected with the indicated epitope-tagged constructs were seeded on glass coverslips 24 h before fixation in 4% paraformaldehyde in PBS for 15 min. After the cells were washed with PBS, blocking and permeabilization were performed for 30 min in PBS containing 10% (v/v) normal goat serum (Sigma, Taufkirchen, Germany), 0.2% (w/v) bovine serum albumin (Sigma), and 0.3% (v/v) Triton X-100. The primary antibodies (rat monoclonal anti-HA (Roche, Mannheim, Germany) and mouse monoclonal anti-V5 (Invitrogen; Karlsruhe, Germany) were diluted in the blocking solution (anti-HA 1/400, anti-V5 1/2000) and incubated with the cells overnight at 4°C. After the cells were washed with PBS, secondary Cy-2- or Cy-3-coupled antibodies (Amersham Pharmacia Biotech, Freiburg, Germany) were added at the recommended dilutions for 2 h at room temperature. Afterward the cells were again washed with PBS and mounted with glycerol-gelatin (Sigma). Epifluorescence microscopy was used to detect antibody localization. A similar procedure was used for immunostaining of 5 µm cryosections of *Xenopus* oocytes, which were fixed over night at 4°C in 4% paraformaldehyde/PBS prior to embedding (Tissue-Tek, Miles, Plano W. Plannet, Wetzlar, Germany) and cutting. Staining of non-permeabilized MDCK cells was achieved by direct addition of the primary antibody to the cell culture medium at room temperature for 2 h. After several washes with PBS, the cells were fixed and processed as described above. For immunoprecipitation oocytes were homogenized in lysis buffer containing 150 mM NaCl, 20 mM TRIS-Cl pH 7.6, 1% Triton X-100. Proteases were inhibited with Complete (Roche) at the recommended concentration. Primary antibody (mouse monoclonal anti V5, Invitrogen) was added overnight at 4°C and subsequently bound to protein G agarose (Roche) at 4°C for 2 h. After several washes, the agarose pellet was solubilized in sample buffer (60 mM TRIS-Cl, 2.3% SDS, 10% glycerol, 0.4% bromphenol-blue, 5% mercaptoethanol) and the supernatant was separated on 8% polyacrylamide gel. Proteins were transferred to nitrocellulose membranes in ice-cold transfer buffer (11.3 g/l glycine, 2.4 g/l TRIS) at 100 V for 90 min. For immunodetection, rat monoclonal anti-HA (1/1000) was added to the blocking solution (5% non-fat milk powder in TBS-Tween: 150 mM NaCl, 25 mM Tris pH 7.4, Tween 20 0.1%) and incubated with the blot for 2 h at room temperature. Secondary peroxidase-conjugated goat anti-rat IgG (1/2000; Jackson ImmunoResearch, Dianova, Hamburg, Germany) was used for luminescent detection with ECL Plus (Amersham).

In situ hybridization

In situ hybridization was performed on 14 µm cryosections of rat kidney using DIG-labeled rat barttin, ClC-K1, and ClC-K2 antisense and sense cRNA probes (DIG-labeling system, Roche). To preclude cross-reactivity, the ClC-K1 and ClC-K2 probes were directed against the non-homologous 3′-untranslated regions of the respective genes. For the generation of the rat barttin probe, the complete rat barttin cDNA was cloned by homology PCR and 5′- and 3′-RACE. The sequence was submitted to GenBank (GenBank Accession Number AJ421029).

Microdissection of nephron segments

Nephron segments for RT-PCR were obtained by a modified collagenase digestion protocol from freshly prepared rat kidney slices [11]. At least 11 mm of each tubule segment was pooled and used for RNA preparation. After cDNA synthesis, PCR was performed on cDNA samples corresponding to 1 mm initial tubule length derived from at least three different sets of nephron segments from different animals. Parallel amplifications of marker genes (NKCC2, AQP-1, AQP-4, PHrP-R) served as controls for the segment specificity of the preparation.

Results

When expressed alone, ClC-Ka-, ClC-Kb- and barttin-induced currents were not significantly different from those in non-injected oocytes. Expression of ClC-Ka together with barttin, however, resulted in large instantaneous currents with a reversal potential close to –20 mV, which showed some voltage-dependent gating in the negative voltage range below –80 mV (Fig. 1A, B). Small but significant currents with voltage-dependent activation in the positive voltage range and inactivation in the negative voltage range were observed after expression of barttin with ClC-Kb (Fig. 1C, D).

Partial replacement of extracellular chloride by other anions indicated a $Cl^- = Br^- > NO_3^- = I^-$ conductance sequence for ClC-Ka+barttin currents, whereas ClC-Kb+barttin currents showed a $Cl^- > Br^- > NO_3^- = I^-$ conductance sequence (Fig. 2A, D). Comparable to rat ClC-K1-currents, the amplitude of ClC-Ka+barttin and ClC-

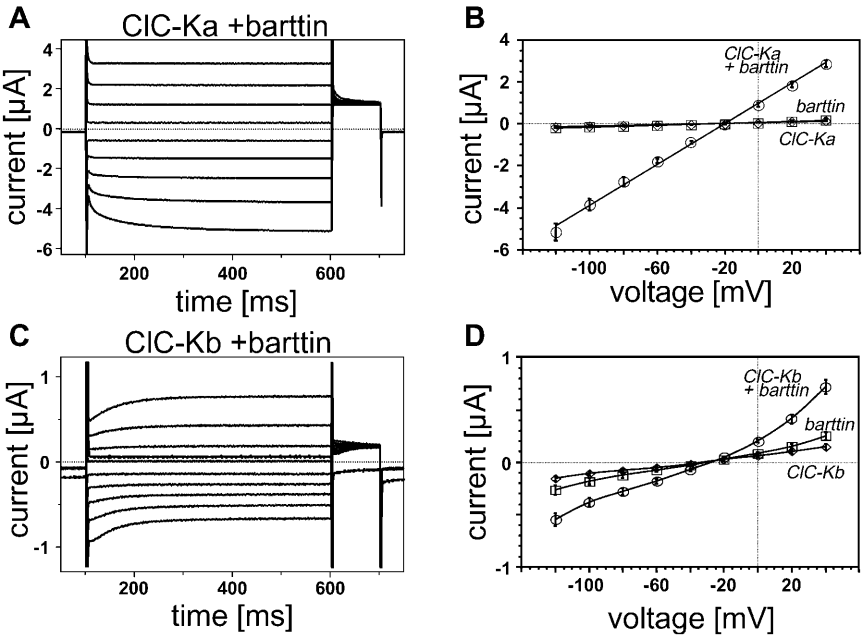

Fig. 1A–D Activation of ClC-K currents by barttin. Two-electrode voltage-clamp traces of currents from *Xenopus* oocytes injected with cRNAs encoding barttin and ClC-Ka (**A**) or ClC-Kb (**C**). Voltage was clamped between –120 and +40 mV and changed in 20-mV steps. The *gray current trace* in **C** was recorded at +40 mV after replacement of extracellular chloride by aspartate. Averaged current/voltage relationships for barttin (**B**, **D**; *squares*; *n*=8), ClC-Ka (**B**; *diamonds*; *n*=8), ClC-Kb (**D**; *diamonds*; *n*=9), ClC-Ka+barttin (**B**; *circles*; *n*=8), and ClC-Kb+barttin (**D**; *circles*; *n*=9)

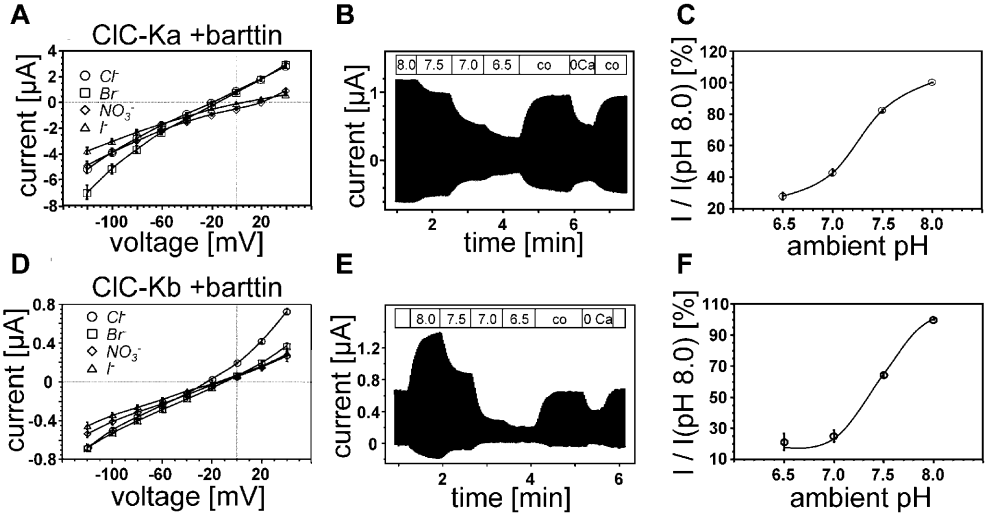

Fig. 2A–F Characterization of ClC-K+barttin channel properties. Current/voltage relationships under control conditions (Cl^-) and after substitution of 80 mM chloride by the indicated anions for ClC-Ka+barttin (**A**; *n*=7) and ClC-Kb+barttin (**D**; *n*=7). Original recordings showing the dependence on extracellular pH and calcium concentration of ClC-Ka+barttin (**B**) and ClC-Kb+barttin (**E**). Currents were recorded during continuous 500-ms voltage steps from –30 to 0 mV at 0.5 Hz. (*co* Control condition at pH 7.4 and 1.8 mM extracellular calcium concentration.) Relative pH effect on ClC-Ka+barttin (**C**; *n*=7) and ClC-Kb+barttin (**F**; *n*=8)

Kb+barttin currents strongly decreased upon extracellular acidification and removal of extracellular calcium (Fig. 2B, E). Compared with ClC-Ka+barttin, ClC-Kb+barttin pH sensitivity was shifted in the alkaline direction (Fig. 2C, F).

To investigate whether the barttin effect was limited to ClC-K channels, we co-expressed barttin and ClC-5, another chloride channel of the CLC-family predominantly expressed in the kidney. Similar to a previous report [17], the expression of ClC-5 gave rise to outwardly rectifying currents, which showed no apparent alterations in the presence of barttin (682±76 nA versus 510±47 nA at +20 mV; *n*=6). Moreover, co-expression of barttin and ROMK, another ion channel associated with Bartter syndrome, did not reveal any differences compared to inwardly rectifying potassium currents generated by ROMK alone (–7.4±0.9 µA and –6.9±0.8 µA respectively at –20 mV and an extracellular KCl concentration of 100 mM; *n*=6).

To test whether barttin changed the biophysical characteristics of ClC-K currents in addition to increasing current amplitude, we expressed barttin together with ClC-K1 and compared current properties with those previously determined for ClC-K1 alone. Comparable to previous reports [20, 23], voltage-clamp analysis of ClC-K1-expressing oocytes revealed small instantaneous chloride currents, which were absent in control oocytes or oocytes injected with barttin cRNA (Fig. 3A, C). A dramatic increase in current amplitude (about 20-fold) was observed after expression of ClC-K1 together with barttin (Fig. 3B, C). Biophysical properties previously reported for ClC-K1 chloride currents include a $Cl^-=Br^->NO_3^-=I^-$ anion permeability sequence and a strong dependence on extracellular pH as well as extracellular calcium concentration

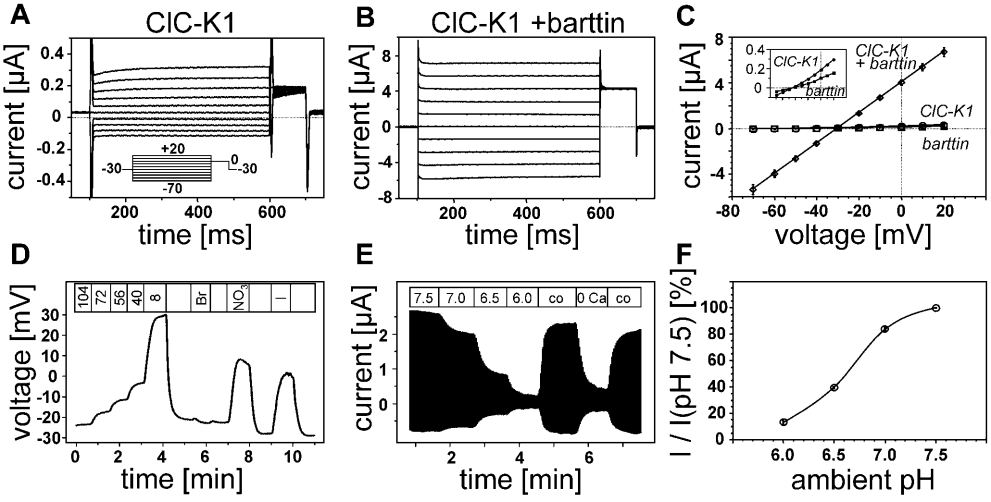

Fig. 3A–F Activation of ClC-K1 currents by barttin. Two-electrode voltage-clamp traces of *Xenopus* oocytes injected with cRNA encoding ClC-K1 (**A**), and ClCK1+barttin (**B**). Voltage was clamped between –70 and +20 mV (**A**, *inset*). **C** Averaged current/voltage relationships for barttin (*squares*), ClC-K1 (*circles*), and ClC-K1+barttin (*diamonds*). Currents were averaged from *n*=7 oocytes. A magnification of the low current range is provided (**C**, *inset*). Characterization of ClC-K1+barttin. **D** Voltage trace at different extracellular chloride concentrations (replacement of chloride by aspartate; the remaining chloride concentration in mM is indicated) and after replacement of 80 mM chloride by the indicated anions. **E** Original tracing showing current amplitude during extracellular acidification from pH 7.5 to 6.0 and removal of extracellular calcium (*0 Ca*). (*co* ND96 at pH 7.4.) Currents were recorded during continuous 500-ms voltage steps from –30 to 0 mV at 0.5 Hz. **F** Relative inhibition of ClC-K1+barttin currents by extracellular acidification (*n*=7)

Fig. 4 Effect of extracellular calcium on ClC-K1 (**A**) and ClC-K1+barttin (**B**). Original current recordings during continuous 500-ms voltage steps from –30 to +20 mV at 0.5 Hz. **C** Relative effect of extracellular calcium on ClC-K1 and ClC-K1+barttin current amplitude (*n*=7). **D** Co-immunoprecipitation of ClC-K isoforms by barttin. The *left panel* shows anti-HA staining of lysates of oocytes expressing V5 barttin (*b*), HA-ClC-Ka (*Ka*), and HA-ClC-Kb (*Kb*). The *right blot* shows anti-HA staining of proteins precipitated by an anti-V5 antibody from lysates of oocytes expressing HA-ClC-K1 (*K1*), HA-ClC-K1+V5-barttin (*K1/b*), the human isoforms HA-ClC-Ka (*Ka*) and HA-ClC-Kb (*Kb*) with or without V5-barttin (*b*), and V5 barttin alone (*b*). The *arrow* points to a ≅250-kDa band which is only present in cells expressing CLC-K together with barttin. A protein band of similar size is visible in the lysates of HA-ClC-Ka- and HA-ClC-Kb-expressing cells, but is absent in V5-barttin-expressing cells, thus demonstrating specificity of the staining. A faint signal is also observed without anti-V5 antibody after control immunoprecipitation of HA-ClC-Kb- and V5-barttin-expressing cells, thus reflecting weak unspecific binding of HA-ClC-K to the precipitating protein G agarose (Kb/b–ab). The intense bands on the right blot at ≅80 and 50 kDa correspond to the heavy and light chains respectively of the precipitating anti-V5 antibody

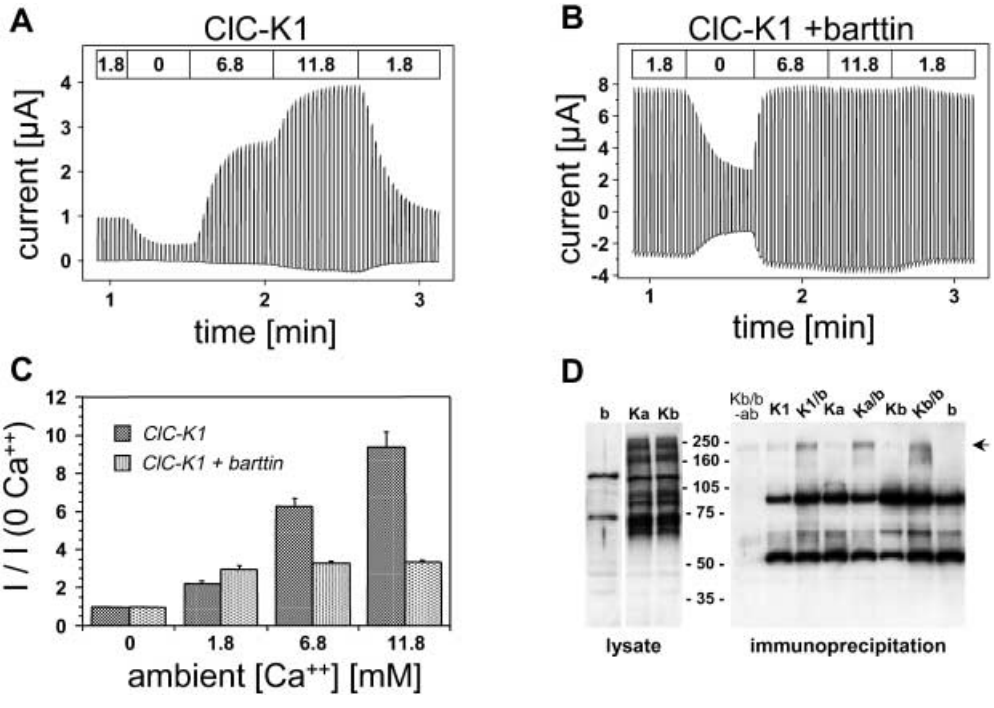

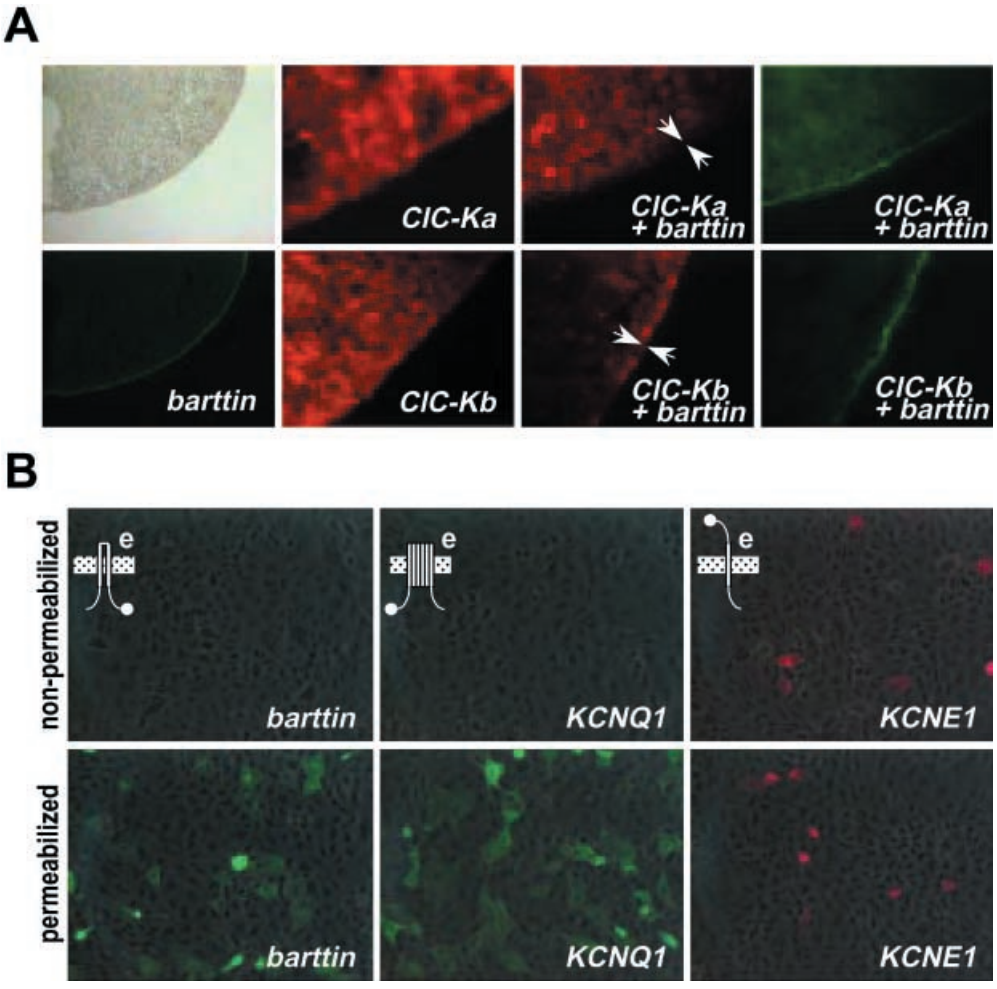

Fig. 5 Immunostaining of barttin and ClC-K in *Xenopus* oocytes (**A**) and localization of the barttin C-terminus in MDCK cells (**B**). *Green staining* in **A** corresponds to V5-tagged barttin, whereas *red staining* corresponds to HA-ClC-Ka or HA-ClC-Kb. The *arrows* point to a surface signal for ClC-Ka and ClC-Kb in oocytes co-expressing barttin. In **B** immunostaining for epitope-tagged barttin, KCNQ1 and KCNE1 is shown before and after permeabilization of transiently transfected MDCK cells. The position of the epitope is marked by the *circles* in the protein models. (*e* Extracellular)

[20, 23]. In a first step, we determined the anion permeability of oocytes co-injected with ClC-K1- and barttin cRNA. As illustrated in Fig. 3D, extracellular replacement of chloride by aspartate resulted in a positive shift of the membrane voltage. This shift with an amplitude of about 50 mV per decade change of extracellular chloride concentration pointed to a selective chloride conductance. Reversal potential measurements after partial replacement of chloride by other anions revealed a $Cl^- = Br^- > NO_3^- = I^-$ permeability sequence identical to that reported for ClC-K1 (Fig. 3D). Again comparable to ClC-K1, ClC-K1+barttin-induced currents rapidly and reversibly decreased upon extracellular acidification (Fig. 3E, F) and removal of extracellular calcium (Fig. 3E). An increase in extracellular calcium concentration to 6.8 and 11.8 mM strongly activated ClC-K1-induced currents (Fig. 4A, C). By contrast, ClC-K1+barttin showed maximal current amplitudes under control conditions (1.8 mM calcium) which could not be further activated by an extracellular calcium increase (Fig. 4B, C). This difference in calcium sensitivity suggested a direct modification of ClC-K channels by barttin.

To test for a direct interaction of barttin with ClC-K proteins, we performed co-immunoprecipitation experiments on lysates of oocytes injected with epitope-tagged ClC-K and barttin constructs. Epitope tagging (N-terminal HA epitope for ClC-K and C-terminal V5 epitope for barttin) did not interfere with the described barttin effect on ClC-K currents (data not shown). Comparable to a previous report [23], the expression of HA-ClC-Ka and HA-ClC-Kb gave rise to several protein bands ranging between 75 and 250 kDa, which were absent in non-injected and V5-barttin injected oocytes and may be explained by glycosylation or denaturation-resistant aggregation of ClC-K proteins. As shown in Fig. 4D, the 250-kDa ClC-K protein fraction selectively immunoprecipitated with V5-barttin in lysates of oocytes co-expressing ClC-K1, ClC-Ka, and ClC-Kb.

We used the same epitope-tagged constructs to investigate the cellular distribution of ClC-K and barttin in *Xenopus* oocytes. When expressed alone, barttin showed a predominant staining in the oocyte plasma membrane, whereas ClC-Ka and ClC-Kb were detected exclusively in the cytosolic compartment (Fig. 5A). Expression of barttin together with ClC-Ka or ClC-Kb led to faint ClC-K signals in the plasma membrane, which – corresponding to the higher current amplitudes – were more pronounced in ClC-Ka-co-expressing oocytes. The barttin distribution pattern was not changed by co-expression of ClC-Ka or ClC-Kb (Fig. 5A).

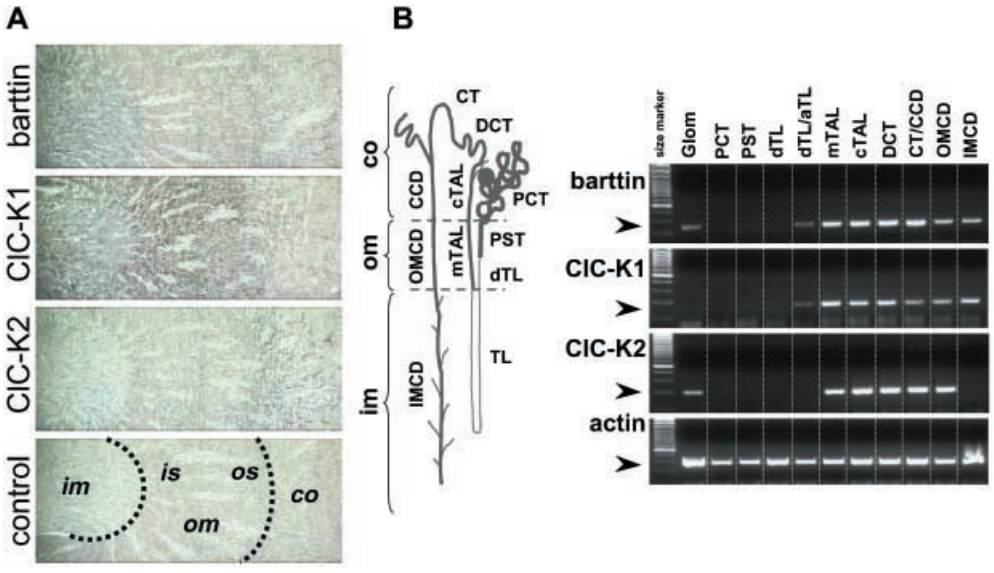

Fig. 6A, B Localization of barttin, ClC-K1, and ClC-K2 in the rat kidney. **A** In situ hybridization on rat kidney cryosections. A positive hybridization signal is indicated by a dark precipitate. Hybridization with the corresponding sense cRNAs served as control. The barttin sense control is shown. (*im* Inner medulla, *om* outer medulla with is inner stripe, *os* outer stripe, *co* cortex.) **B** RT-PCR experiments on microdissected tubule segments of rat kidney. The *arrowheads* point to the amplification products of the expected size. The positive signal in the glomerulus in the case of barttin and ClC-K2 may derive from adherent structures of the distal convoluted tubule (juxtaglomerular apparatus). A nephron with the corresponding tubule segments is shown schematically. (*aTL* Ascending thin limb, *CCD* cortical collecting duct, *CT* connecting tubule, *cTAL* cortical thick ascending limb, *DCT* distal convoluted tubule, *dTL* descending thin limb, *Glom* glomerulus, *IMCD* inner medullary collecting duct, *mTAL* medullary thick ascending limb, *OMCD* outer medullary collecting duct, *PCT* proximal convoluted tubule, *PST* proximal straight tubule)

Algorithmic topology prediction suggested a short intracellular N-terminus (eight amino acids), two transmembrane domains connected by a short linker (five amino acids), and a long intracellular C-terminus (266 amino acids) for the barttin protein. In addition to hydrophobic interaction of the integral membrane part of barttin with ClC-K proteins, the long C-terminal protein region could form a potential interaction domain. The intracellular localization of the ClC-K N- and C-terminal protein regions [12] would require a similar orientation of the barttin C-terminus for protein–protein interaction. We therefore determined the orientation of the barttin C-terminus in MDCK cells transfected with the C-terminal V5-tagged barttin construct. As shown in Fig. 5B, similar to the intracellularly tagged KCNQ1 protein [18], staining of the C-terminal barttin V5-epitope was only detected after permeabilization of the transfected MDCK cells. By contrast, extracellularly tagged KCNE1 [18] was also stained in non-permeabilized cells. This confirmed the predicted intracellular localization of the barttin C-terminus.

As deduced from morphological studies, barttin and ClC-K are expressed in the distal nephron. To substantiate the co-expression of barttin and ClC-K transcripts, we performed in situ hybridizations on rat kidney slices. As illustrated in Fig. 6A, hybridization with a rat barttin probe gave rise to distinct signals throughout the inner medulla. A somewhat weaker staining was observed in most of the tubular parts of the outer medulla and in scattered tubule segments of the cortex. A similar distribution pattern was found for ClC-K1 transcripts, whereas ClC-K2 was absent in the inner medulla and only faintly expressed in the inner stripe of the outer medulla. Prominent expression of ClC-K2 was restricted to the outer stripe of the outer medulla and to scattered cortical tubule segments that most likely corresponded to those positive for barttin and ClC-K1. In agreement with these data, PCR experiments on microdissected nephron segments revealed the expression of ClC-K1 and barttin throughout the distal nephron including tubule segments of the inner medulla (thin limb of the loop of Henle and inner medullary collecting duct). ClC-K2 expression was limited to outer medullary nephron segments (medullary thick ascending limb and outer medullary collecting duct) and cortical parts of the distal nephron (cortical thick ascending limb, distal convolute, connecting tubule, and cortical collecting duct) (Fig. 6B).

The results reported here suggest that ClC-K activation by barttin forms the molecular basis of BSND. BSND-associated point mutations hence should impair the barttin effect on ClC-K. Mutational analysis of the BSND gene revealed, in addition to several nonsense mutations, three homozygous missense mutations affecting amino acids 8 and 10 at the border to the first putative transmembrane domain [2]. We tested their functional relevance by co-expression with ClC-K1 in *Xenopus* oocytes. As expected, the R8L and R8W mutations nearly completely abolished ClC-K1 activation by barttin (Fig. 7). The barttin G10S mutant, however, still activated ClC-K1 to an extent similar to that of wild-type

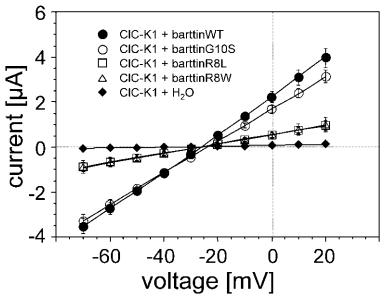

Fig. 7 Effect of BSND-associated barttin mutations on ClC-K1 activation. Current/voltage relationships are shown for oocytes injected with 1 ng ClC-K1 cRNA alone (*filled diamonds*; *n*=7) or together with 0.5 ng cRNA encoding barttin wild-type (*WT*, *filled circles*; *n*=10), barttin G10S mutant (*open circles*; *n*=8), barttin R8L mutant (*open squares*; *n*=7), and barttin R8W mutant (*open triangles*; *n*=7)

barttin. Differences in cellular protein quality control mechanisms or in protein targeting mechanisms between the *Xenopus* oocyte and the native barttin-expressing cells may explain this discrepancy.

Discussion

Our work describes the activation of ClC-K chloride channels by an accessory protein, which increases ClC-K abundance in the cell membrane. A similar observation was recently published by another group [5]. Deduced from compelling co-localization of barttin and ClC-K proteins in the distal nephron and in endolymph-producing cells of the inner ear, the authors of that study postulated a direct interaction of ClC-K and barttin in a heteromeric channel structure. The here-reported change in ClC-K1 calcium sensitivity after co-expression with barttin supports this hypothesis and indicates that increased ClC-K surface expression is not the only mechanism responsible for ClC-K current activation. However, although enhanced surface expression and altered biophysical properties were reported to be indicators of the heteromeric assembly of other ion channels [13, 25], alternative mechanisms for barttin-mediated channel modulation could be imagined. Barttin, for example, could act as a scaffolding protein directing endogenous proteins to the cell membrane, which in turn could modify ClC-K proteins. We therefore sought to directly demonstrate an interaction between barttin and ClC-K in co-immunoprecipitation experiments, which indeed revealed stable association of these proteins. Barttin hence forms an integral part of the functional ClC-K channel. In view of the unaffected anion selectivity, however, the direct participation of barttin in the ClC-K pore structure seems unlikely.

Barttin is localized in strial marginal cells of the cochlea and in vestibular dark cells [2, 5], which were also shown to express ClC-K in their basolateral membranes [5, 10]. The primary function of both cell types is to secrete potassium into the endolymph space. This process requires in addition to an apical potassium conductance (mediated by KCNQ1/KCNE1 channels) a large basolateral chloride conductance, which recycles chloride taken up by a parallel sodium-potassium-chloride co-transport mechanism (mediated by the NKCC1 cotransporter). Analogous to an insufficiency in endolymph secretion after KCNQ1 [3], KCNE1 [22] or NKCC1 [4] gene deletion in mouse models, impaired ClC-K activity in BSND patients may disturb endolymph production and hence lead to sensorineural deafness. A similar mechanism was proposed for hearing loss of patients suffering from Jervell and Lange–Nielsen syndrome, which is caused by loss of function mutations in KCNQ1 or KCNE1 [9].

In the kidney our in situ hybridization and RT-PCR experiments revealed co-localization of barttin and ClC-K1 throughout the distal nephron starting with the thin limb of Henle's loop. This agrees with the distribution pattern of barttin mRNA described in the original cloning report and with several ClC-K1 localization studies based on microdissection techniques [7, 19, 21]. With an immunofluorescence approach, ClC-K1 was detected only in the thin limb of Henle's loop [20], which, however, might be put down to different sensitivities of the applied techniques. In the case of ClC-K2, our localization to outer medullary and cortical tubule segments of the distal nephron confirms a previous expression study [24]. Exclusive expression of barttin and ClC-K1 thus is limited to the thin limb of Henle's loop and the inner medullary collecting duct, whereas in all other segments of the distal nephron an overlapping expression is found for ClC-K1, ClC-K2 and barttin. The distal nephrons are the main site of transcellular chloride reabsorption. A serial arrangement of apical and basolateral ClC-K1 chloride channels was implied in passive chloride reabsorption in the thin ascending limb. Transepithelial chloride absorption in this nephron segment is an important component of the countercurrent system and contributes to the high inner medullary tonicity required for urinary concentration. In support of this notion the targeted inactivation of ClC-K1 in a mouse model was shown to result in a nephrogenic *diabetes-insipidus*-like phenotype due to impaired inner medullary solute accumulation [1, 8]. By contrast, ClC-K2/Kb was suggested as the basolateral chloride release pathway in the thick ascending limb and in more distal tubule segments. Disturbances in this part of the nephron are causally related to the tubular salt wasting in Bartter syndrome. Therefore, in the case of a mere impairment of ClC-K1/Ka activity by mutations in barttin, one would expect an increase in water diuresis rather than in salt diuresis. On the other hand, an isolated impairment of ClC-Kb activity, as is the case in classic Bartter syndrome (cBS), is associated with a relatively mild phenotype with only partially disturbed urine concentrating ability. The severe salt-losing phenotype of BSND patients thus argues for a combined impairment of ClC-Ka and ClC-Kb activity. Indeed, similar to the cBS caused by mutations in ClC-Kb, BSND patients escape nephrocalcinosis [6], a typical complication of

the other Bartter variants. Moreover, the more severe phenotype of BSND as compared to cBS argues for the additional involvement of ClC-K1/Ka in the etiology of the renal salt wasting.

In conclusion we have shown that barttin is an activator of ClC-K chloride channels. ClC-K activation by barttin is associated with an increase in membrane abundance and alteration of the extracellular calcium sensitivity of ClC-K channels. As deduced from the BSND phenotype, barttin-mediated ClC-K activation is a prerequisite for normal hearing, probably via the control of endolymph homeostasis, and adequate chloride reabsorption along the distal nephron. In addition to detailed insights into the pathological mechanisms of a new variant of Bartter syndrome, this study opens the field of CLC channel regulation by accessory protein subunits.

Acknowledgements We thank Hayo Castrop for scientific discussion and support in the microdissection experiments. This work was supported by the Deutsche Forschungsgemeinschaft (WA 1088/3–1 to S.W.), the Kempkes foundation of the university of Marburg, and a research grant from Aventis.

References

1. Akizuki S, Uchida S, Sasaki S, Marumo F (2001) Impaired solute accumulation in inner medulla of *Clcnk1-/-* mice kidney. Am J Physiol 280:F79–F87
2. Birkenhäger R, Otto E, Schürmann MJ, Vollmer M, Ruf E-M, Maier-Lutz I, Beekmann F, Fekete A, Omran H, Feldmann D, Milford DV, Jeck N, Konrad M, Landau D, Knoers NVAM, Antignac C, Sudbrak R, Kispert A, Hildebrandt F (2001) Mutation of *BSND* causes Bartter syndrome with sensorineural deafness and kidney failure. Nature Genet 29:310–314
3. Casimiro MC, Knollmann BC, Ebert SN, Vary JC, Greene AE, Franz MR, Grinberg A, Huang SP, Pfeifer K (2001) Targeted disruption of the KCNQ1 gene produces a mouse model of Jervell and Lange-Nielsen syndrome. Proc Natl Acad Sci USA 98:2526–2531
4. Delpire E, Lu J, England R, Dull C, Thorne T (1999) Deafness and imbalance associated with inactivation of the secretory Na-K-2Cl co-transporter. Nature Genet 22:192–195
5. Estevez R, Boettger T, Stein V, Birkenhäger R, Otto E, Hildebrandt F, Jentsch TJ (2001) Barttin is a Cl^- channel beta-subunit crucial for renal Cl^- reabsorption and inner ear K^+ secretion. Nature 414:558–561
6. Jeck N, Reinalter SC, Henne T, Marg W, Mallmann R, Pasel K, Vollmer M, Klaus G, Leonhardt A, Seyberth HW, Konrad M (2001) Hypokalemic salt-losing tubulopathy with chronic renal failure and sensorineural deafness. Pediatrics 108:E5
7. Kieferle S, Fong P, Bens M, Vandewalle A, Jentsch TJ (1994) Two highly homologous members of the ClC chloride channel family in both rat and human kidney. Proc Natl Acad Sci USA 91:6943–6947
8. Matsumura Y, Uchida S, Kondo Y, Miyazaki H, Ko SBH, Hayama A, Morimoto T, Liu W, Arisawa M, Sasaki S, Marumo F (1999) Overt nephrogenic diabetes insipidus in mice lacking the CLC-K1 chloride channel. Nature Genet 21:95–98
9. Neyroud N, Tesson F, Denjoy I, Leibovici M, Donger C, Barhanin J, Faure S, Gary F, Coumel P, Petit C, Schwartz K, Guicheney P (1997) A novel mutation in the potassium channel gene KVLQT1 causes the Jervell and Lange-Nielsen cardioauditory syndrome. Nature Genet 15:186–189
10. Sage CL, Marcus DC (2001) Immunolocalization of ClC-K chloride channel in strial marginal cells and vestibular dark cells. Hear Res 160:1–9
11. Schäfer JA, Watkins ML, Li L, Herter P, Haxelmans S, Schlatter E (1997) A simplified method for isolation of large numbers of defined nephron segments. Am J Physiol 273:F650–F657
12. Schmidt-Rose T, Jentsch TJ (1997) Transmembrane topology of a CLC chloride channel. Proc Natl Acad Sci USA 94:7633–7638
13. Schroeder B, Waldegger S, Fehr S, Bleich M, Warth R, Greger R, Jentsch T (2000) A constitutively open potassium channel formed by KCNQ1 and KCNE3. Nature 403:196–199
14. Simon DB, Bindra RS, Mansfield TA, Nelson-Williams C, Mendonca E, Stone R, Schurman S, Nayir A, Alpay H, Bakkaloglu A, Rodriguez-Soriano J, Morales JM, Sanjad SA, Taylor CM, Pilz D, Brem A, Trachtman H, Griswold W, Richard GA, John E, Lifton RP (1997) Mutations in the chloride channel gene, *CLCNKB*, cause Bartter's syndrome type III. Nature Genet 17:171–178
15. Simon DB, Karet FE, Hamdan JM, Di Pietro A, Sanjad SA, Lifton RP (1996) Bartter's syndrome, hypokalaemic alkalosis with hypercalciuria, is caused by mutations in the Na-K-2Cl cotransporter NKCC2. Nature Genet 13:183–188
16. Simon DB, Karet FE, Rodriguez-Soriano J, Hamdan JH, DiPietro A, Trachtman H, Sanjad SA, Lifton RP (1996) Genetic heterogeneity of Bartter's syndrome revealed by mutations in the K^+ channel, ROMK. Nature Genet 14:152–156
17. Steinmeyer K, Schwappach B, Bens M, Vandewalle A, Jentsch TJ (1995) Cloning and functional expression of rat ClC-5, a chloride channel related to kidney disease. J Biol Chem 270:31172–31177
18. Suessbrich H, Busch AE (1999) The IKs channel: coassembly of IsK (minK) and KvLQT1 proteins. Rev Physiol Biochem Pharmacol 137:191–226
19. Uchida S, Sasaki S, Furukawa T, Hiraoka M, Imai T, Hirata Y, Marumo F (1993) Molecular cloning of a chloride channel that is regulated by dehydration and expressed predominantly in kidney medulla. J Biol Chem 268:3821–3824
20. Uchida S, Sasaki S, Nitta K, Uchida K, Horita S, Nihei H, Marumo F (1995) Localization and functional characterization of rat kidney-specific chloride channel, ClC-K1. J Clin Invest 95:104–113
21. Vandewalle A, Cluzeaud F, Bens M, Kieferle S, Steinmeyer K, Jentsch TJ (1997) Localization and induction by dehydration of ClC-K chloride channels in the rat kidney. Am J Physiol 272:F678–F688
22. Vetter DE, Mann JR, Wangemann P, Liu J, McLaughlin KJ, Lesage F, Marcus DC, Lazdunski M, Heinemann SF, Barhanin J (1996) Inner ear defects induced by null mutation of the isk gene. Neuron 17:1251–1264
23. Waldegger S, Jentsch TJ (2000) Functional and structural analysis of ClC-K chloride channels involved in renal disease. J Biol Chem 275:24527–24533
24. Yoshikawa M, Uchida S, Yamauchi A, Miyai A, Tanaka Y, Sasaki S, Marumo F (1999) Localization of rat CLC-K2 chloride channel mRNA in the kidney. Am J Physiol 276:F552–F558
25. Zerangue N, Schwappach B, Jan Y, Jan L (1999) A new ER trafficking signal regulates the subunit stoichiometry of plasma membrane K(ATP) channels. Neuron 22:537–548